Effect of Anodizing Time and Annealing Temperature on Photoelectrochemical Properties of Anodized TiO$_2$ Nanotube for Corrosion Prevention Application

Misriyani[1,*], Abdul Wahid Wahab[2], Paulina Taba[2], and Jarnuzi Gunlazuardi[3]

[1]Medical Education, Faculty of Medicine, University of Alkhairaat,
Jl. Diponegoro Palu 94221, Central Sulawesi, Indonesia

[2]Department of Chemistry, Faculty of Mathematics and Natural Sciences, Hasanuddin University,
Jl. Perintis Kemerdekaan 90245, Makassar-Indonesia

[3]Department of Chemistry, Faculty of Mathematics and Natural Sciences, Universitas Indonesia,
Depok 16424, Indonesia

ABSTRACT

A study on the influence of anodizing time, annealing temperature and photoelectrochemical properties of TiO$_2$ nanotube (TiO$_2$ NT) has been investigated. The crystallinity was investigated using X-Ray Diffraction and the anti-corrosion performance of stainless steel 304 (SS 304) coupled with TiO$_2$ NT was evaluated using electrochemical techniques under ultraviolet exposure. The optimum anodizing condition occurs at a voltage of 20 V for 3 h. After anodizing, the TiO$_2$ NT amorf was calcined at 500 °C to obtain anatase crystalline phase. For the photoelectrochemical property, the effects of pH and NaCl concentration on corrosion prevention have been examined. The result showed that the corrosion rate of stainless steel 304 coupled with TiO$_2$ NT can be reduced up to 1.7 times compared to the uncoupled stainless steel 304 (3.05×10^{-6} to 1.78×10^{-6} mpy) under ultraviolet exposure by shifted the photopotential to the more negative value (-0.302 V to -0.354 V) at a pH of 8 and 3% NaCl concentration (-0.264 V to -0.291 V). In conclusion, the TiO$_2$ NT films, which was prepared by anodization and followed by annealing can prevent the corrosion of stainless steel 304.

Keywords: anodizing time; annealing temperature; pH; stainless steel 304

ABSTRAK

Studi tentang pengaruh waktu anodisasi, suhu kalsinasi dan sifat fotoelektrokimia TiO$_2$ nanotube (TiO$_2$ NT) telah diteliti. Kristalinitas sampel dianalisis dengan menggunakan Difraksi Sinar X dan kinerja anti-korosi stainless steel 304 yang dicopel dengan TiO$_2$ NT dievaluasi dengan menggunakan teknik elektrokimia pada paparan sinar ultraviolet. Kondisi anodisasi optimum terjadi pada tegangan 20 V selama 3 jam. Setelah anodisasi, TiO$_2$ NT amorf dikalsinasi pada suhu 500 °C untuk mendapatkan kristal fasa anatase. Sifat fotoelektrokimia, pengaruh pH dan konsentrasi NaCl pada pencegahan korosi telah diteliti. Hasil penelitian menunjukkan bahwa laju korosi dari stainless steel 304 yang dikombinasikan dengan TiO$_2$ NT menurun hingga 1,7 kali dibandingkan dengan stainless steel tanpa copel TiO$_2$ NT ($3,05 \times 10^{-6}$ menjadi $1,78 \times 10^{-6}$ mpy) pada paparan sinar ultraviolet dengan menggeser photopotential ke arah nilai yang lebih negatif (-0,302 V ke -0,354 V) pada pH 8 dan konsentrasi NaCl 3% (-0,264 V ke -0,291 V). Kesimpulannya, film TiO$_2$ NT, yang dipreparasi dengan metode anodisasi dan diikuti oleh pemanasan dapat mencegah korosi stainless steel 304.

Kata Kunci: waktu anodisasi; suhu pemanasan; pH; stainless steel 304

INTRODUCTION

Titanium dioxide (TiO$_2$) is a semiconductor material that is very important and has many benefits. In the last few years, TiO$_2$ gives a great attention due to its ability to be used as photocatalyst materials, non toxic, self cleaning, sollar cells, gas sensing and corrosion-resistant material with over 5000 publications that have been produced [1-2]. TiO$_2$ in the micro powder form has a limitation to be used for the above application due to its low surface area, so that large amount of TiO$_2$ is required for those applications as has been postulated by Misriyani et al. [3]. This problem can be solved by converting the particle form to the nanotubular form. According to Roy et al. [4], the nanotubular form has higher surface area than the particle form.

TiO$_2$ NT have been prepared by various method such as hydrothermal treatment [5-6], template

---

deposition [7-8] and electrochemical anodizing method [9-11]. Anodization with electrochemical method using titanium foil in fluoride that containing electrolyte has been chosen as the favorable method because the surface of TiO_2 NT films have formed a strong bond with the titanium subtrate. It is also a low cost and simple method [1,12]. Kapusta-Kołodziej et al. [13] reported that the effectiveness of TiO_2 NT depends evidently on TiO_2 layers. The layers of TiO_2 NT can be controlled by several parameters such as electrolyte concentration, pH, temperature, anodizing voltage, anodizing time and calcination temperature [14]. In addition, as we know that anodized titania nanotube are amorphous that can transform to crystalline by thermal treatment. This study aimed to understand the anodization time and annealing temperature parameters that affecting the TiO_2 surface properties by investigating its crystalline properties.

The applications of TiO_2 NT as corrosion resistance material have been reported by many researches. One application was the use of TiO_2 NT for cathodic protection of steel under UV illumination [15-17]. However, the works provide limited information of the influence of the electrolyte conditions to corrosion properties. Liu et al. [18] and Wang et al. [19] has reported that the corrosion resistance of steel was affected by pH and concentration of electrolytes. This paper reported the influence of the two parameters on the corrosion properties of SS304 coupled with TiO_2 NT under UV illumination. The linear sweep voltammetry, multi pulse amperometry and polarization curve were used to discuss the photoelectrochemical activity and corrosion rate of TiO_2 NT.

EXPERIMENTAL SECTION

Materials

The TiO_2 nanotube films were grown on the surface of the titanium foil as substrate (Baoji Jinsheng Metal Material Co., purity 99.6 %, thickness 0.3 mm) by anodization method using glycerol 98% p.a (Merck), Ammonium Fluoride (NH_4F) (Merck) and connected with two electrode cells. Sodium chloride (Merck) was used as corrodes electrolyte solution, while sodium oxalate (Merck) was used as electrolyte solution for photoelectrochemical analysis of TiO_2 nanotube, NaOH (Merck) and HNO_3 (Merck) were used to make the pH series, as well as abrasive paper, distilled water, acetone and ethanol was used as washing solvent.

Instrumentation

Anodization process was conducted using power supply (BK-Precision DC) to provide DC current. The e-DAQ potentiostat connected with computer device

(eCHEM software) to record the result of electrochemical analysis. Characterization of the crystalline structure was measured using an X-Ray Diffraction instrument with Cu kα radiation at 40 kV and 30mA (Maxima.X Shimadzu).

Procedure

Preparation of TiO_2 nanotube

Titanium foils were polished by #1000 and #400 abrasive paper and ultrasonically cleaned for 30 min in acetone, ethanol and deionized water. Afterwards, anodization was carried out using electrode cells for 0; 1; 2 and 3 h in glycerol based electrolyte containing 0.5% NH_4F and 25% distilled H_2O at a potential of 20 V (power supply BK-Precision DC) between titanium foils as anode with a fixed distance of 2 cm and Pt foils as cathode cell [20]. In order to change the form of sample from amorphous to crystalline, the thermal treatment at 400, 500, 600 and 700 °C was conducted in a furnace (Barnstead Thermolyne Analytical Lab). The temperature was increased from room temperature to the certain temperature and maintained at the temperature for 3 h.

Photoelectrochemical characterization of TiO_2 nanotube

Photocurrent were measured using three electrode cell connected to potentiostat eDAQ (model ED401) and UV lamp 11W GNB model as a source of illumination. The TiO_2 NT was used as a working electrode, platinum as a counter electrode and Ag/AgCl as reference electrode. The experiments were carried out in HCOONa (0.05 M) electrolyte with potential range ± 1.2 V at a constant scan rate of 10 mV/s, in the dark and under illumination to get the photocurrent density value using a linear sweep voltammetry technique. For the corrosion test, photoelectrochemical system was performed at two compartments; TiO_2 NT as a working electrode in the photoanode cell and the

1. Ti Substrate
2. TiO_2 nanotube
3. Stainless Steel
4. Ag/AgCl electrode
5. Graphite carbon
6. Salt bridge
7. Formate solution
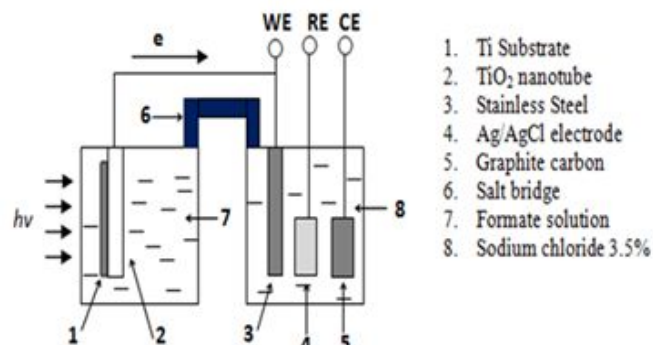8. Sodium chloride 3.5%

Fig 1. Photoelectrochemical system for corrosion prevention [30,17]

other as the corrosion cell at the cathode cell consisted of stainless steel, counter and reference electrodes. The two cell compartments were connected by an external circuit as shown in Fig. 1 and the electrolyte were connected by a salt bridge (U pipe containing KCl in agar). NaCl solution was used as electrolyte at corrosion cell that prepared with concentration varying between 3 to 4 M.

RESULT AND DISCUSSION

Characterization

Effect of calcination temperature

Fig. 2 shows the X-ray diffraction pattern of TiO_2 NT at calcination temperature of 400; 500; 600 and 700 °C. At these patterns, the four samples of TiO_2 NT provide a good peak character of TiO_2 anatase and rutil. The characteristic of the peak for anatase phase is at $2\theta = 25°, 36°, 48°$. Whereas the one for rutile phase is at $2\theta = 27°$. The peak for anatase phase appears in the four diffractograms. The intensity of peak in diffractogram (b) 500 °C is considered higher than that in other diffractogram. At the heating temperature of 400 °C the peak for anatase and rutile phase is not too intense. It indicates that the phase is still dominated by amorphous [10]. The intensity of the phase increases at heating temperature of 500 °C. The increase in intensity of the anatase peak is very high, whereas the rutile phase is low. At the heating temperature of (c) 600 and (d) 700 °C the peak intensity of anatase phase drastically decreases.

During the calcination process, porous titanium dioxide undergoes crystallization process to form anatase and rutile phase depending on the annealing temperature, as can be seen in the XRD spectra. In this study, the peak intensity of the anatase increases with calcination temperature up to 500 °C, indicating that the anatase crystallization increases with increasing calcination temperature [21]. However, when heatead increased up to 700 °C, the intensity of the anatase decreases, followed by the appearance of rutile peak. Similar observation was also reported by Sreekantan et al. [22].

Effect of anodizing time

Fig. 3 shows the diffractograms of TiO_2 NT at anodizing time of 0 h; 1 h; 2 h; and 3 h. The XRD pattern showed that unanodized material (0 h anodizing), only provide titanium character peaks at $2\theta = 37; 39$ and $52°$, while the TiO_2 character peaks have not been detected. After the anodizing process and thermal treatment at 500 °C, the anatase characters peak appear at $2\theta = 25°; 36°; 37°; 38°; 48°$ and $54°$ according to Zhang et al. [23]. The titanium peak at $38.4°$ (002); $40.4°$ (101) and $53.2°$
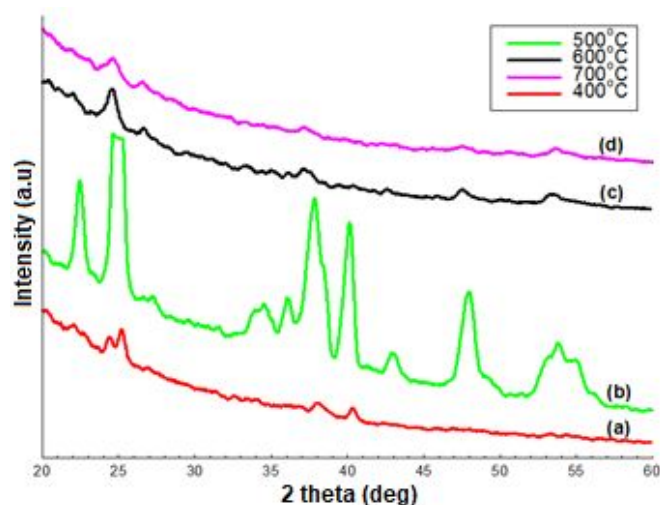

Fig 2. X-ray diffractogram of TiO_2 NT at temperature calcination: (a) 400 °C; (b) 500 °C; (c) 600 °C; and (d) 700 °C
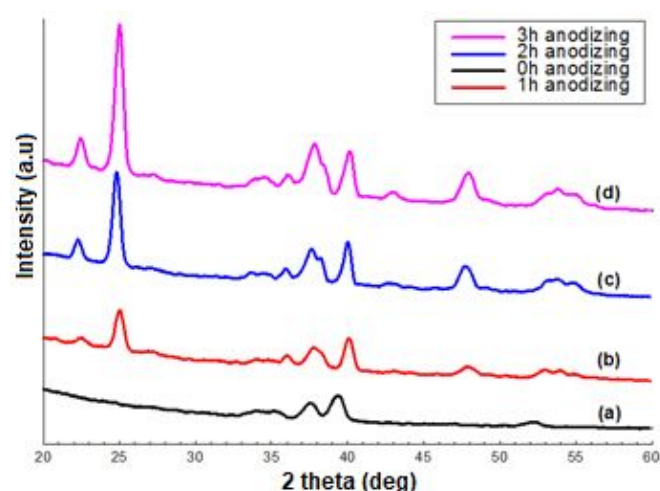

Fig 3. X-ray diffractogram of TiO_2 NT of (a) unanodized and (b, c, d) anodized at 1 h, 2 h and 3 h, respectively

(102) become weak and lost, this indicates that the substrate of titanium has been oxidized during anodization and transformed to crystal phase during the heating process at the temperature of 500 °C.

The intensity of anatase peak increases by increasing the anodizing time. The increase of intensity may be resulted by the increase of tube length. Our previous work reports in detail the growth of tubes of TiO_2 nanotube with the average length 3.4 nm [24]. Li et al. [25] reported that the long process of anodizing could increase the length of the tube that increase the thickness of TiO_2 NT. Bauer et al. [2] and Nischk et al. [11] report that the growth of thickness of nanotube film could increase the intensity of the peak of anatase. It is also influenced by the amount of surface area of TiO_2 NT in the material.
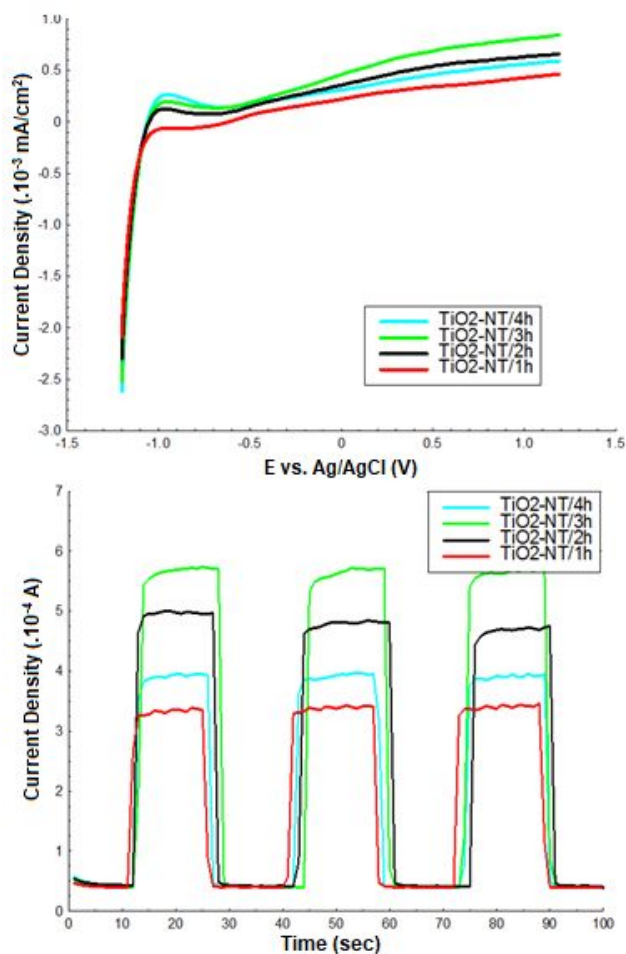
222

Indones. J. Chem., 2017, 17 (2), 219 - 227

Fig 4. Photocurrent response curves of TiO₂ NT with techniques: a) linear sweep voltammetry; b) Multi Pulse amperometry on UV light exposure

Fig 5. Photocurrent response curves of TiO₂ NT with techniques: a) linear sweep voltammetry; b) Multi Pulse amperometry on UV light exposure

Photoelectrochemical Test

Effect of anodizing time

The influence of anodizing voltage on photoelectrochemical behavior of TiO₂ NT has been discussed in the previous study [26]. As has been mention above that anodizing time was also important in the formation of the nanotube. The anodizing time affected the tube length, while anodizing voltage affected the tube diameter. Fig. 4 shows photocurrents of TiO₂ NT as a function of the anodizing time. It can be seen that the increase of anodizing time is in accordance with the increase of photocurrent. This shows that the tube length increases with the increase of the time of anodizing. The increase of tube length may increase the contact of light with the surface of TiO₂ NT films, as has been postulated by Acevedo-Peña and González [27]. Kim et al. [28] reported that the surface area of the TiO₂
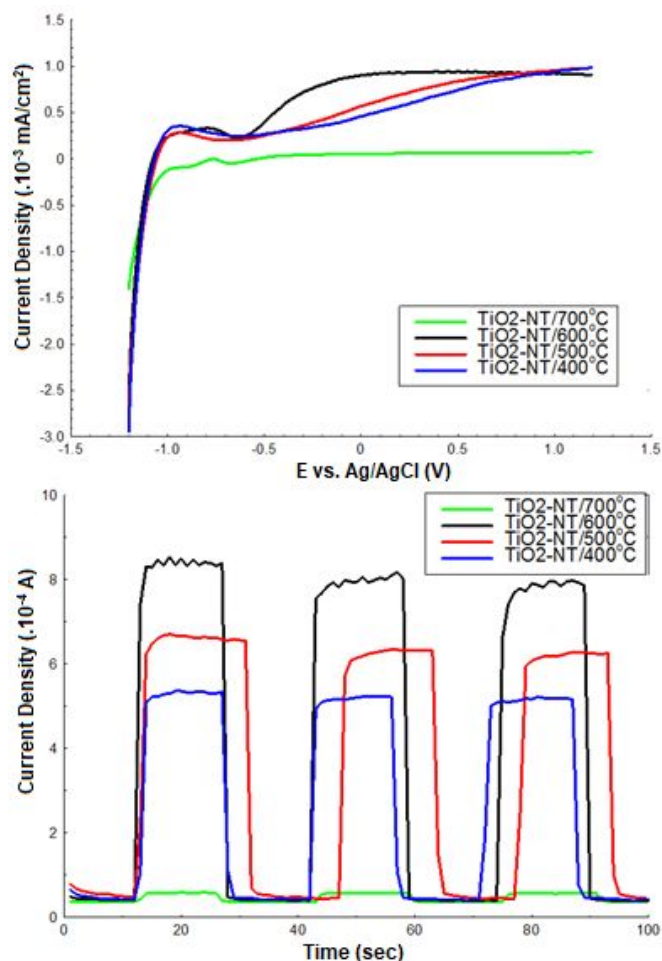
NT increases with the increase of the tube length. Therefore, photoelectrochemical activity increases.

In addition, the higher the tube length, the greater possibility of the tube wall to be contacted with titanium substrate due to the increase of charge transport electricity and the small resistance between TiO₂ NT and titanium substrate. Photocurrent and light response decrease at anodizing time of 4 hours, as shown in the multi pulse amperometry curve (Fig. 4b). The reduction of photoelectrochemical activity was caused by the damage of surface due to the long chemical etching process. The damage surface of the tube causes the increase of recombinant between the excited electrons and the hole. Thereby the values of current density of the light response decrease. This result is supported by the result of Xing et al. [29]. In addition, the tube wall thickness decreases by increasing anodizing time. As a result, the active surface area of TiO₂ NT decreases. The same result has been reported by Li et al. [10].
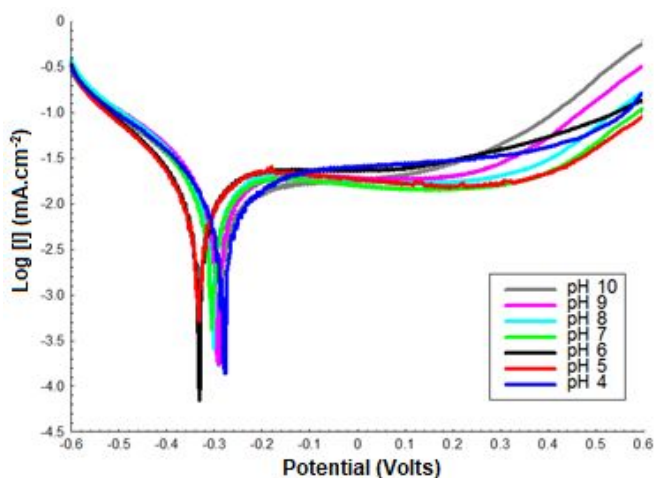
Fig 6. Tafel polarization curve of stainless steel at variation of pH in NaCl solution

Fig 7. Effect of pH to corrosion potential shifts of stainless steel couple with TiO_2 NT on dark and UV light exposure

Effect of calcination temperature

Fig. 5 shows the photocurrent response of TiO_2 NT as a function of the calcination temperature. It is obvious that TiO_2 NT calcined at 500 °C provides the highest photocurrent density, because a lot of electrons can be transported during the UV light exposure. According to Li et al. [10], it can be resulted from the excellent crystalline and the well order nanotubular structure that very useful as a charge transfer place.

Fig. 5b shows the multi pulse amperometry curve to determine the photoelectrochemical activity. This result indicated the good response of TiO_2 NT to UV light exposure. Therefore it is useful to be applied as anti corrosion material on stainless steel.

Anti Corrosion Test

Effect of pH

The mechanism of corrosion prevention of metal refers to previous study which reported that on photocathode system, the excitation of electrons of TiO_2 nanotube will occur under ultraviolet light exposure. Furthermore, the electrons will flow on the metal and shifting the metal potential to more negative values. The accumulation of electrons on the surface of the metal causing the metal can be protected from oxidation, so that corrosion prevention of metal can be achieved [30-32]. Analysis of corrosion prevention mechanism of TiO_2 nanotube material can be determined by computing QSAR method or molecular dynamic study. It allows to predict the potential inhibition and anticorrosion properties in some of material [33-35], which was not reported in this paper.

Fig. 6 shows Tafel polarization curve of stainless steel in the variation of pH at 3.5% NaCl solution. It can be observed that the potential value is closed to the positive 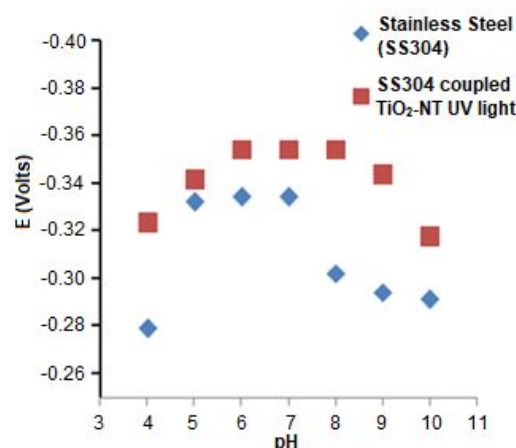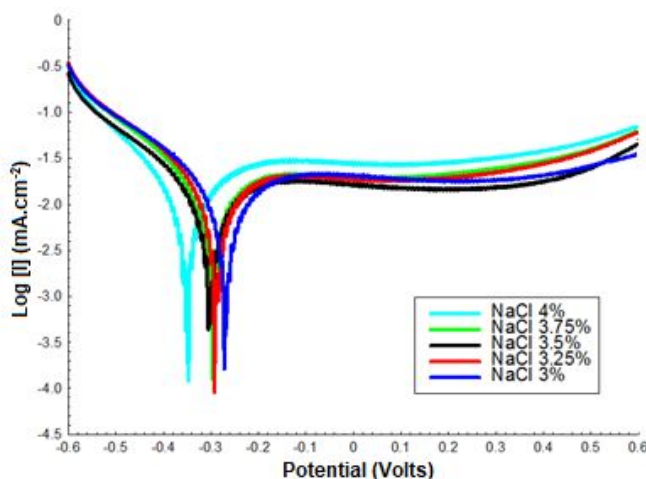value provide by the solution at pH 4. The increased pH, decreases the corrosion potential value towards the more negative until pH 6. The pH 6 give the most negative corrosion potential than others, which indicates the most optimum conditions to protect stainless steel from corrosion. Furthermore the increasing pH up to 10, increase the potential value towards the more positive value until pH 10. From the above result it can concluded that the corrosion occurs at more acidic or more alkaline of NaCl solution.

Fig. 7 shows the TiO_2 NT prevent the corrosion stainless steel at varying pH. It can be observed that for overall pH value, the potential value of stainless steel coupled with TiO_2 NT shifts to the more negative (accordance with as shown in Table 1). It indicates that stainless steel coupled with TiO_2 NT have been successfully protected the stainless steel from corrosion. The potential corrosion of stainless steel coupled with TiO_2 NT in more acidic or more alkaline condition shows more positive potential. This indicates that, at this condition, the stainless steel is vulnerable to corrosion.

The electrochemical parameters obtained from analytical calculations of polarization curves showed at Table 1. The Icorr, Ecorr and corr rate parameters, which indicates the current density, corrosion potential and the corrosion rate of stainless steel coupled and uncoupled with TiO_2 NT respectively. The corrosion rate of stainless steel coupled with TiO_2 NT under ultraviolet exposure at a pH of 8 decreases up to 1.7 times that of uncoupled stainless steel. However the corrosion rate of stainless steel coupled with TiO_2 NT at other pH is higher than that of uncoupled stainless steel. This indicates that there is no protection for the corrosion of stainless steel. It concluded that the corrosion prevention of stainless steel by using TiO_2 NT can be performed in NaCl solution at pH 8. The result

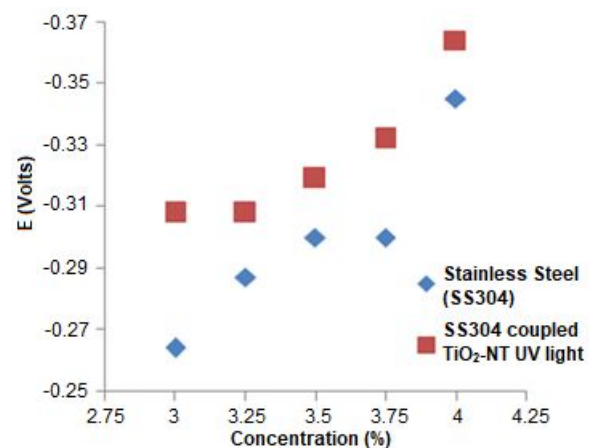**Table 1.** Electrochemical parameters at different pH of NaCl solution

Sample	pH values	E_{corr}	I	Corr.rate
		V	A cm^{-2}	mpy
Stainless steel 304	10	-0.291	5.51 x 10-7	6.40 x 10^{-6}
	9	-0.294	1.92 x 10^{-7}	2.23 x 10^{-6}
	8	-0.302	2.63 x 10^{-7}	3.05 x 10^{-6}
	7	-0.334	1.42 x 10^{-7}	1.65 x 10^{-6}
	6	-0.334	2.75 x 10^{-7}	3.20 x 10^{-6}
	5	-0.332	5.15 x 10^{-7}	5.98 x 10^{-6}
	4	-0.279	3.79 x 10^{-7}	4.40 x 10^{-6}
SS + TiO$_2$-NT UV	10	-0.317	1.2 x 10^{-6}	1.40 x 10^{-5}
	9	-0.343	3.30 x 10^{-7}	3.83 x 10^{-6}
	8	-0.354	1.54 x 10^{-7}	1.78 x 10^{-6}
	7	-0.354	2.21 x 10^{-7}	2.57 x 10^{-6}
	6	-0.354	5.72 x 10^{-7}	6.64 x 10^{-6}
	5	-0.341	8.22 x 10^{-7}	9.55 x 10^{-6}
	4	-0.323	1.22 x 10^{-6}	1.42 x 10^{-5}

Fig 8. Tafel polarization curve of stainless steel on variations of NaCl solution concentration

Fig 9. Effect of NaCl concentrations to corrosion potential shifts of stainless steel couple with TiO$_2$ NT on dark and UV light exposure

is supported by the most significant shift of potential value of SS 304 coupled with TiO$_2$ NT compare to SS 304 at pH 8.

Effect of NaCl concentration

Fig. 8 shows the tafel polarization curve of stainless steel in various concentrations of NaCl solution. It can be observed that potential value of stainless steel shifts toward the more negative value by increasing the concentration of NaCl. This indicates that the best corrosion protection occurs at high NaCl concentrations of 3%. The existence of chloride ions influences the corrosion process. The result is not parallel with the one reported by Wang et al. [19] and Asaduzzaman et al. [36]. According to the researches the higher the concentration of NaCl, increase the rate of corrosion reaction and shift the potential to the more negative value. The opposite result obtained in this study is possibly caused by the high concentration of Cl$^-$ which

was above the threshold value. According to Eliyan et al. [37], it can decrease the corrosion rate and it can control the rate of corrosion by cathodic reaction.

Liu et al. [38] also reported that increasing Cl$^-$ concentration up to maximum value of 2.5% can promote the anodic reaction and inhibit the cathodic reaction. At Cl$^-$ concentration more than 2.5%, the corrosion was controlled by cathodic reaction during corrosion process. As a consequence, the corrosion potential value shifted to the more negative direction or the corrosion was protected. It is accordance with the Cl$^-$ concentration range used in this study from 3–4%.

Fig. 9 shows the influence of NaCl concentration on corrosion potential shift of stainless steel coupled with TiO$_2$ NT on UV light exposure. In addition the corrosion rate of stainless steel coupled with TiO$_2$ NT decrease up to 2.2 times compare with uncoupled stanless steel at 3% NaCl concentration as shown in Table 2. It is clear that stainless steel coupled with TiO$_2$

Table 2. Electrochemical parameters at different NaCl concentration

Sample	Concentration	E_{corr}	I	Corr.rate
		V	A cm^{-2}	mpy
Stainless steel 304	4 %	-0.347	1.19×10^{-7}	6.40×10^{-6}
	3.75 %	-0.300	6.26×10^{-7}	2.23×10^{-6}
	3.5 %	-0.300	5.11×10^{-7}	3.05×10^{-6}
	3.25 %	-0.287	1.37×10^{-6}	1.59×10^{-5}
	3 %	-0.264	1.73×10^{-6}	2.01×10^{-5}
SS + TiO$_2$-NT UV	4 %	-0.364	1.29×10^{-6}	1.50×10^{-5}
	3.75 %	-0.332	1.96×10^{-7}	2.28×10^{-6}
	3.5 %	-0.319	2.49×10^{-8}	2.89×10^{-7}
	3.25 %	-0.308	6.52×10^{-7}	7.57×10^{-6}
	3 %	-0.308	7.90×10^{-7}	9.18×10^{-6}

NT can protect the stainless steel from corrosion by shifting the corrosion potential towards the more negative value and also decrease the corrosion rate. The significant potential shift occurs at 3% NaCl (from -0.264 V to -0.291 V) which indicate the highest performance of TiO$_2$ NT to prevent the corrosion under UV light exposure.

CONCLUSION

The TiO$_2$ NT can be obtained by anodizing process at anodizing time of 3 h followed by thermal treatment at 500 °C. The tube length and crystallinity increase with the applied anodizing time and calcination temperature. The photoelectrochemical measurements showed that the stainless steel 304 coupled with TiO$_2$ NT could shift the corrosion potential to the more negative value under UV light exposure, with the significant potential shift occur at pH 8 and 3% NaCl concentration. In addition the corrosion rate of stainless steel 304 coupled with TiO$_2$ NT can reduce up to 1.7 times and 2.2 times compare to bare stainless steel at pH 8 and 3% NaCl concentration respectively. In conclusion the TiO$_2$ NT can reduce the corrosion rate of stainless steel 304 and the result is expected to be used as a reference conditions chosen for preventing the corrosion from the environment.

ACKNOWLEDGEMENT

REFERENCES

[1] Li, L., Zhou, Z., Lei, J., He, J., Zhang, S., and Pan, F., 2012, Highly ordered anodic TiO$_2$ nanotube arrays and their stabilities as photo(electro)catalysts, *Appl. Surf. Sci.*, 258 (8), 3647–3651.

[2] Bauer, S., Pittrof, A., Tsuchiya, H., and Schmuki, P., 2011, Size-effects in TiO$_2$ nanotubes: Diameter dependent anatase/rutile stabilization, *Electrochem. Commun.*, 13 (6), 538–541.

[3] Misriyani, Kunarti, E.S., and Yasuda, M., 2015, Synthesis of Mn(II)-loaded Tl$_x$Si$_{1-x}$O$_4$ composite acting as a visible-light driven photocatalyst, *Indones. J. Chem.*, 15 (1), 43–49.

[4] Roy, P., Berger, S., and Schmuki, P., 2011, TiO$_2$ nanotubes: Synthesis and applications, *Angew. Chem. Int. Ed.*, 50 (13), 2904–2939.

[5] Vuong, D.D., Tram, D.T.N., Pho, P.Q., and Chien, N.D., 2009, "Hydrothermal Synthesis and Photocatalytic Properties of TiO$_2$ Nanotubes" in *Physics and Engineering of New Materials*, 95–101.

[6] Lee, C.H., Kim, K.H., Jang, K.U., Park, S.J., and Choi, H.W., 2011, Synthesis of TiO$_2$ Nanotube by Hydrothermal Method and Application for Dye-Sensitized Solar Cell, *Mol. Cryst. Liq. Cryst.*, 539 (1), 125/[465]–132/[472].

[7] Qiu, J., Yu, W., Gao, X., and Li, X., 2006, Sol–gel assisted ZnO nanorod array template to synthesize TiO$_2$ nanotube arrays, *Nanotechnology*, 17 (18), 4695–4698.

[8] Koh, J.H., Koh, J.K., Seo, J.A., Shin, J.S., and Kim, J.H., 2011, Fabrication of 3D interconnected porous TiO$_2$ nanotubes templated by poly(vinyl chloride-g-4-vinyl pyridine) for dye-sensitized solar cells, *Nanotechnology*, 22 (36), 365401.

[9] Yoriya, S., Kittimeteeworakul, W., and Punprasert, N., 2012, Effect of anodization parameters on morphologies of TiO$_2$ nanotube arrays and their surface properties, *J. Chem. Chem. Eng.*, 6 (8), 686–691.

[10] Li, Y., Yu, H., Zhang, C., Song, W., Li, G., Shao, Z., and Yi, B., 2013, Effect of water and annealing temperature of anodized TiO$_2$ nanotubes on hydrogen production in photoelectrochemical cell, *Electrochim. Acta*, 107, 313–319.

[11] Nischk, M., Mazierski, P., Gazda, M., and Zaleska, A., 2014, Ordered TiO$_2$ nanotubes: The effect of

preparation parameters on the photocatalytic activity in air purification process, *Appl. Catal., B*, 144, 674–685.

[12] Lee, B.G., Choi, J.W., Lee, S.E., Jeong, Y.S., Oh, H.J., and Chi, C.S., 2009, Formation behavior of anodic TiO_2 nanotubes in fluoride containing electrolytes, *Trans. Nonferrous Met. Soc. China*, 19 (4), 842–845.

[13] Kapusta-Kołodziej, J., Tynkevych, O., Pawlik, A., Jarosz, M., Mech, J., and Sulka, G.D., 2014, Electrochemical growth of porous titanium dioxide in a glycerol-based electrolyte at different temperatures, *Electrochim. Acta*, 144, 127–135.

[14] Omidvar, H., Goodarzi, S., Seif, A., and Azadmehr, A.R., 2011, Influence of anodization parameters on the morphology of TiO_2 nanotube arrays, *Superlattices Microstruct.*, 50 (1), 26–39.

[15] Lei, C.X., Zhou, H., Wang, C., and Feng, Z.D., 2013, Self-assembly of ordered mesoporous TiO_2 thin films as photoanodes for cathodic protection of stainless steel, *Electrochim. Acta*, 87, 245–249.

[16] Shen, G.X., Chen, Y.C., and Lin, C.J., 2005, Corrosion protection of 316L stainless steel by a TiO_2 nanoparticle coating prepared by sol–gel method, *Thin Solid Films*, 489, (1-2), 130–136.

[17] Park, H., Kim, K.Y., and Choi, W., 2002, Photoelectrochemical approach for metal corrosion prevention using a semiconductor photoanode, *J. Phys. Chem. B*, 106 (18), 4775–4781.

[18] Liu, Q.Y., Mao, L.J., and Zhou, S.W., 2014, Effects of chloride content on CO_2 corrosion of carbon steel in simulated oil and gas well environments, *Corros. Sci.*, 84, 165–171.

[19] Wang, Y., Cheng, G., Wu, W., Qiao, Q., Li, Y., and Li, X., 2015, Effect of pH and chloride on the micro-mechanism of pitting corrosion for high strength pipeline steel in aerated NaCl solutions, *Appl. Surf. Sci.*, 349, 746–756.

[20] Misriyani, Wahab, A.W., Taba, P., and Gunlazuardi, J., 2015, Synthesis of TiO_2 nanotube decorated Ag as photoelectrode: Application for corrosion prevention of stainless steel 304 under visible light exposure, *Int. J. Appl. Chem.*, 11 (5), 611–619.

[21] Hu, J., Shaokang, G., Zhang, C., Ren, C., Wen, C., Zeng, Z., and Peng, L., 2009, Corrosion protection of AZ31 magnesium alloy by a TiO_2 coating prepared by LPD method, *Surf. Coat. Technol.*, 203 (14), 2017–2020.

[22] Sreekantan, S., Lockman, Z., Hazan, R., Tasbihi, M., Tong, L.K., and Mohamed, A.R., 2009, Influence of electrolyte pH on TiO_2 nanotube formation by Ti anodization, *J. Alloys Compd.*, 485 (1-2), 478–483.

[23] Zhang, J., Du, R., Lin, Z., Zhu, Y., Guo, Y., Qi, H., Xu, L., and Lin, C., 2012, Highly efficient CdSe/CdS co-sensitized TiO_2 nanotube films for photocathodic

protection of stainless steel, *Electrochim. Acta*, 83, 59–64.

[24] Misriyani, Wahab, A.W., Gunlazuardi, J., Taba, P., and Shiomori, K., 2015, Synthesis and characterization of TiO_2 nanotube films for a photo-electrochemical corrosion prevention of stainless steel under UV light exposure, *Int. J. Appl. Chem.* 11 (4), 443–453.

[25] Li, S., Liu, Y., Zhang, G., Zhao, X., and Yin, J., 2011, The role of the TiO_2 nanotube array morphologies in the dye-sensitized solar cells, *Thin Solid Films*, 520 (2), 689–693.

[26] Misriyani, Kunarti, E.S., and Yasuda, M., 2015, Synthesis of Mn(II)-loaded $Ti_xSi_{1-x}O_4$ composite acting as a visible-light driven photocatalyst, *Indones. J. Chem.*, 15 (1), 43–49.

[27] Acevedo-Peña, P., and González, I., 2014, Relation between morphology and photoelectrochemical performance of TiO_2 nanotubes arrays grown in ethylene glycol/water, *Procedia Chem.*, 12, 34–40.

[28] Kim, K.P., Lee, S.J., Kim, D.H., Hwang, D.K., and Heo, Y.W., 2013, Dye-sensitized solar cells based on trench structured TiO_2 nanotubes in Ti substrate, *Curr. Appl. Phys.*, 13 (4), 795–798.

[29] Xing, J., Li, H., Xia, Z., Chen, J., Zhang, Y., and Zhong, L., 2014, Influence of substrate morphology on the growth and properties of TiO_2 nanotubes in HBF_4-based electrolyte, *Electrochim Acta*, 134, 242–248.

[30] Lei, C.X., Zhou, H., Feng, Z.D., Zhu, Y.F., and Du, R.G., 2012, Liquid phase deposition (LPD) of TiO_2 thin films as photoanodes for cathodic protection of stainless steel, *J. Alloys Compd.*, 513, 552–558.

[31] Yu, D., Wang, J., Tian, J., Xu, X., Dai, J., and Wang, X., 2013, Preparation and characterization of TiO_2/ZnO composite coating on carbon steel surface and its anticorrosive behavior in seawater, *Composites Part B*, 46, 135–144.

[32] Cui, S., Yin, X., Yu, Q., Liu, Y., Wang, D., and Zhou, F., 2015, Polypyrrole nanowire/TiO_2 nanotube nanocomposites as photoanodes for photocathodic protection of Ti substrate and 304 stainless steel under visible light, *Corros. Sci.*, 98, 471–477.

[33] Eddy, N.O., and Ita, B.I., 2011, QSAR, DFT and quantum chemical studies on the inhibition potentials of some carbozones for the corrosion of mild steel in HCl, *J. Mol. Model.*, 17 (2), 359–376.

[34] Hadanu, R., Idris, S., and Sutapa, I.W., 2015, QSAR analysis of benzothiazole derivatives of antimalarial compounds based on AM1 semi-empirical method, *Indones. J. Chem.*, 15 (1), 86–92.

[35] Wang, H., Liu, L., Huang, Y., Wang, D., Hu, L., and Loy, D.A., 2014, Enhancement corrosion resistance of (γ-glycidyloxypropyl)-silsesquioxane-titanium dioxide films and its validation by gas molecule diffusion coefficients using Molecular Dynamics (MD) simulation, *Polymers*, 6 (2), 300–310.

[36] Asaduzzaman, M.D., Mohammad, C., and Mayeedul, I., 2011, Effects of concentration of sodium chloride solution on the pitting corrosion behavior of AISI 304L austenitic stainless steel, *Chem. Ind. Chem. Eng. Q.*, 17 (4), 477–483.

[37] Eliyan, F.F., Mohammadi, F., and Alfantazi, A., 2012, An electrochemical investigation on the effect of the chloride content on CO_2 corrosion of API-X100 steel, *Corros. Sci.*, 64, 37–43.

[38] Liu, Q.Y., Mao, L.J., and Zhou, S.W., 2014, Effects of chloride content on CO_2 corrosion of carbon steel in simulated oil and gas well environments, *Corros. Sci.*, 84, 165–171.